RSC Advances

ROYAL SOCIETY OF CHEMISTRY

www.rsc.org/advances

RSC Advances

RSCPublishing

ARTICLE

Effect of redox properties of ceria-supported vanadium oxides in the liquid phase cyclohexene oxidation

Cite this: DOI: 10.1039/x0xx00000x

Sanaa EL-KORSO, Sumeya BEDRANE, Abderrahim CHOUKCHOU-BRAHAM*, Redouane BACHIR

Received 04th may 2015,
Accepted 00th …….. 2015

DOI: 10.1039/x0xx00000x

www.rsc.org/

Several VO_2/CeO_2 based catalysts, with V loadings between 5 and 20 wt.%, were prepared by impregnation and subsequently dried, calcined and reduced at 673 K. The structural characterization of these materials was carried out using X-rays diffraction (XRD), N_2 adsorption–desorption at 77 K, UV–vis diffused reflectance spectroscopy (DR UV–vis) and Fourrier-Transformed Infrared Spectroscopy (FTIR). Their catalytic activities in the epoxidation of cyclohexene, with TBHP as oxidant and heptane as solvent, were also examined. XRD results revealed a good dispersion of VO_2 species on ceria. FTIR and DR UV–visible spectroscopy techniques indicated that polymeric vanadyl species are present on all catalysts and a crystalline VO_2 phase appears on the 20 wt.% vanadium sample.
Experimental results pointed out that catalysts activity decreases with increased vanadium loading, whereas the epoxide selectivity increased up to 90 % when vanadia loading reached 15 wt.%. In the case of 20 wt.%VO_2/CeO_2, the reaction switched towards a 100 % enol, enone selectivity. The presence of $CeVO_4$ was shown to influence the conversion and selectivity of the reaction.

1. Introduction

Direct oxidation of hydrocarbons into epoxides is one of the most important reactions because of its numerous applications in organic synthesis, as well as in food, agrochemical and pharmaceutical industries [1, 2]. 1,2-Epoxycyclohexane is an important intermediate in the synthesis of several products, such as enantioselective drugs, epoxy paints, rubber promoters and dyestuff. In general, epoxides can be prepared by oxidation of the corresponding alkenes using hydrogen peroxide or alkylhydroperoxides in the presence of high-valent transition metal catalysts [3].
More recently, for the purpose of a fundamental study, supported vanadium oxide catalysts have received a particular interest; they constitute a model for catalytic systems [4] because of their activity in a wide range of applications [5], such as many oxidation reactions [6].
During the last decade, catalyst scientists have unambiguously shown that the activity and selectivity of supported metal oxide catalysts are significantly affected by the properties of the support oxide material [5]. It has been observed that the selectivity and activity of these catalysts depend on multiple factors, i.e. the vanadium loading, method of support preparation, oxidation state of vanadia in the support, calcination temperature, nature of the support, its surface acidity, etc [7, 8]. Several studies have indicated the extent to which vanadia/support interactions may be influenced by dispersion, surface structures, redox and acid–base properties [9, 10], base [11, 12] and redox properties [13] can be intentionally monitored.

* *Laboratoire de Catalyse et Synthèse en Chimie Organique, Faculté des Sciences, Université de Tlemcen, Algeria. mail : cba@mail.univ-tlemcen.dz*

In fact, using different supports and metal loadings, the surface structure[14, 15], number of surface sites number of surface sites, the acid–base [11, 12] and redox properties [13] can be intentionally monitored. Consequently, considerable attention has been focused on the preparation, characterization and evaluation of vanadium oxide catalysts deposited on various single or mixed oxides. Cerium-based materials were widely used as oxygen carriers [16, 17]. The addition of a low amount of cerium can enhance the oxydo-reduction features of a given catalyst. Generally, the oxidation rate is limited by the oxygen transfer from the metal active sites to the metal/support interface, while ceria is able to enhance this oxygen transfer to efficiently catalyze the reaction. The redox properties of ceria (Ce^{4+}/Ce^{3+}) and the high lability of its lattice oxygen are among the most important factors that contribute to the catalytic reactivity in oxidation reactions[18, 19]. The presence of vanadia on ceria affords interesting performances for oxidative dehydrogenation reactions[20-22]. The surface polymeric vanadia species on ceria are more reducible than the isolated ones, according to *in situ* Raman spectroscopy [23].
In general, interfaces between metal oxides supported on metal oxide substrates (supported on another metal oxide) have been less studied than those between metals supported on metal oxides [24]. It has been established, in our previous studies [25] on the liquid epoxidation reaction over mixed vanadium oxides, that the presence of catalysts with redox features directs the reaction toward epoxidation. However, increasing the strength of Lewis acid sites leads to allylic oxidation.
For the same purpose, we report in the present work the structural characterization of ceria supported vanadia catalysts, for various VO_2 loadings considered, using different physico-chemical techniques. Catalysts activity towards liquid phase epoxidation of

cyclohexene is also investigated and correlated with different vanadia species on the supported catalysts. The effect of reaction parameters such as the catalyst weight, temperature, oxidant concentration, leaching and stability was also checked.

2. Experimental

2.1 Synthesis

2.1.1. Starting materials

The following chemicals were employed in the preparation of X wt.%V/CeO_2: Cerium (IV) oxide (CeO_2; Aldrich), ammonium metavanadate (NH_4VO_3; Strem chemicals, 99 %), nitric acid (Aldrich), cyclohexene (Aldrich 99 %), hydroperoxide tertio-butyl (TBHP, Aldrich 70 %) and heptane (Fluka 99 %).

2.1.2 Synthesis of the system Xwt.%VO_2/CeO_2

Typical procedure for 5 wt.%VO_2/CeO_2**:** the 5 wt.%VO_2/CeO_2 catalyst used in this study was prepared by an impregnation procedure [26]. Prior to impregnation, the CeO_2 support was calcined at 673 K, for 4 h. Ammonium metavanadate (NH_4VO_3) was used as the VO_2 precursor. A volume of 40 mL of nitric acid was added to 0.57 g of ammonium metavanadate and stirred for 2 h, then 4.75 g of CeO_2 were added to this solution. The resulting mixture was stirred for 24 h. It was next dried first at 60 °C for one night, then at 120 °C for another night, and then calcined in air at 400 °C, for 4 h. It was finally reduced, under hydrogen flow, at 400 °C, for 4 h. The materials obtained were green, a color that indicates the presence of reduced vanadium (IV) species [27]. For the other catalysts, amounts of ammonium metavanadate, ceria and nitric acid where recalculated in order to obtain 10, 15 and 20 wt% loadings.
All catalysts under study in this paper are summarized in the following table 1:

All catalysts under study in this paper are summarized in the following table 1:

Table 1: Synthesized catalysts with various thermal treatments

Catalyst	V loading (%)	NH_4VO_3 (g)	CeO_2 (g)	HNO_3 (ml)	Thermal treatment
V_2O_5/CeO_2	5	0.57	4.75	40	4h under air at 400°C
VO_2/CeO_2	5	0.57	4.75	40	4h under air at 400°C + 4h under H_2 at 400°C
VO_2/CeO_2	10	1.13	4.50	80	4h under air at 400°C + 4h under H_2 at 400°C
VO_2/CeO_2	15	1.71	4.25	120	4h under air at 400°C + 4h under H_2 at 400°C
VO_2/CeO_2	20	2.27	4.00	160	4h under air at 400°C + 4h under H_2 at 400°C
VO_2/CeO_2	5	0.57	4.75	80	4h under air at 400°C + 4h under H_2 at 400°C + 4h under Ar at 800°C

2.2. Catalyst characterization

All catalysts were characterized by X-ray powder diffraction (XRD), using a Bruker D5005 diffractometer with Cu Kα radiation (λ = 1.54060 Å), in the range of 2θ = 10 °- 80 °, with a step of 0.02 ° and an acquisition time of 1s. Elemental analysis was performed using atomic absorption with a Perkin Elmer Analyst 300 spectrometer. The prepared samples were analyzed by thermal analysis (TGA / DTA) using an SDT Q600 instrument. The 20-30 mg sample mass was introduced into a platinum crucible, which is supported by the beam of a balance in the oven. The analysis was performed in air with a temperature ramp of 5 K/min in the range 298 - 1473 K. These analyses have been carried out in the Laboratory of Catalysis in Organic Chemistry (LACCO, UMR6503) Poitiers University, France. The BET surface area was determined from N_2 adsorption isotherms at 77 K, using a Quantachrom instrument. Prior to nitrogen adsorption, the sample was out-gassed at 673 K for 3 h, under a 30% nitrogen gas stream in helium. The FT-IR spectra of the solid samples were recorded, using an Agilent Technologies Cary 60 series FT-IR spectrometer, with ATR accessories, within the measuring range of 400 – 4000 cm^{-1}. The UV-visible spectra (200 - 800 nm) of these samples were recorded on a Perkin Elmer UV-VIS Spectrometer with integration sphere. The baseline was recorded, using MgO as reference. The Scanning Electron Microscopy (SEM) with EDX (Energy Dispersive X-ray) analysis was performed using a Hitachi- TM.1000, at a 150 kV acceleration voltage.

2.3. Catalytic experiments

The catalytic epoxidation of cyclohexene, with tertio-butylhydroperoxyde TBHP (Aldrich, 70 wt.% in H_2O) as an oxidant, was carried out in a two-necked glass round-bottom flask equipped with a magnetic stirrer and a reflux condenser. First, TBHP was stirred with heptane as solvent in order to perform a phase transfer from water to organic phase. Typically, 25 mL of heptane and 38.45 mmol of TBHP (5.5 mL) were mixed in a closed Erlenmeyer flask and magnetically stirred for 24 h. The organic phase was then separated from the aqueous phase. To control the phase transfer, the concentration of the remaining TBHP, in the aqueous phase, was determined by iodometric titration. More than 90 % of the initial TBHP is transferred in the organic phase to be used in the catalytic reaction. Secondly, 29 mmol (3 mL) of cyclohexene, 0.1 g of catalyst and the TBHP–heptane mixture (organic phase) were all mixed in a magnetic stirrer-glass reactor at 338 K, during 6 h. The reaction products were identified by comparison with authentic products, and the course of reactions was followed by gas chromatography (GC), using a SCHIMADZU 14-B gas chromatograph equipped with an Agile HP-FFAP capillary column. A flame ionization detector (FID) was used to analyze 0.5 µL of the sample. Before GC analysis, the remaining TBHP was decomposed by introducing an excess of triphenylphosphine (Aldrich). Meanwhile, an iodometric titration was performed at the end of the reaction (after 6 h) in order to control the remaining TBHP in the reaction mixture (results reported as % TBHP consumption in tables 4-8). The catalytic performances were reported in terms of cyclohexene conversion, selectivity towards products and Turnover Frequency. They are calculated following the expressions below:

$$Conv\ (\%) = \frac{moles\ of\ initial\ substrate - moles\ of\ residual\ substrate}{moles\ of\ initial\ substrate} \times 100$$

$$Selectivity\ (\%) = \frac{moles\ of\ individual\ product}{moles\ of\ total\ products} \times 100$$

$$TOF\ (h^{-1}) = \frac{nbr\ epoxide\ molecules}{nbr\ \ V\ sites \times time}$$

3. Results and discussion

3.1. Physico-chemical characterization

3.1.1 Powder XRD analysis

The X-ray reflection peaks of ceria were observed at 2θ ~ 28.57 °, 33.11 °, 47.53 ° and 56.37 ° [ICDD pattern 43-1002], corresponding to Miller indices (111), (200), (220) and (311), respectively (Fig. 1) [28]. This shows a typical crystal structure of the cubic fluorite-type ceria [29]. The diffraction patterns of X wt.%VO_2/CeO_2, calcined and reduced at 673 K, showed lines due to ceria, but no lines characteristic of VO_2 were seen (Fig. 1) [30]. This indicates that vanadia was finely dispersed on the ceria surface for this sample[6, 31, 32].

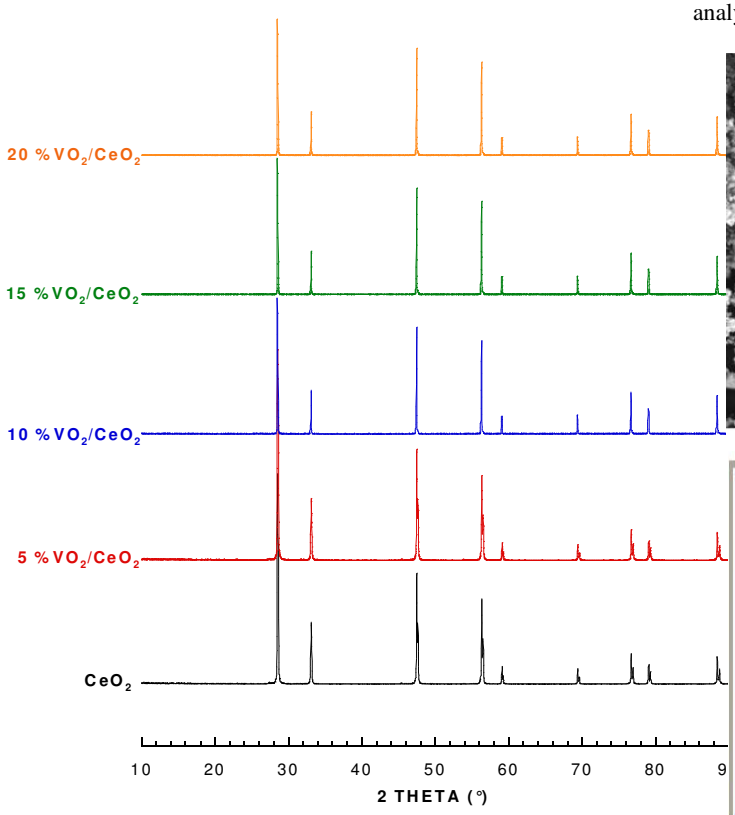

Fig. 1 X-ray diffraction (XRD) patterns of the CeO_2 and X wt.%VO_2/CeO_2 systems.

3.1.2 Surface area measurements

The surface areas of X wt.%VO_2/CeO_2 supported oxides, measured by N_2 adsorption, according to the BET method, are shown in table2. The results show that the commercial ceria, used in this study, has no surface area. However, the latter increases upon impregnation of vanadium oxide on ceria. This phenomenon may be attributed most likely to the vanadium surface area which increases with the vanadium loading. An unusual phenomena of hydration–dissolution and re-precipitation of the support during the preparation procedure has been reported on V/CeO_2 [21] and V/MgO [33] systems. In these cases, the support partly dissolves in the acidic V-containing precursor solution, and then precipitates on evaporation of water, thus generating a V-loaded material with a larger surface area than the initial support. However, it does not seem to be the case here, as the formation of ceria with smaller size should be accompanied by broader XRD peaks.

Table 2 Textural characteristics, as determined by N_2 adsorption, for different samples.

Material	S_{BET} ($m^2\ g^{-1}$)	Pore volume ($cm^3\ g^{-1}$)	Pore size (Å)
CeO_2	01	/	/
5%VO_2/CeO_2	05	0.008	162
10%VO_2/CeO_2	14	0.076	207
20%VO_2/CeO_2	18	0.025	175

3.1.3 Scanning Electron Microscopy (SEM) with EDX

SEM micrographs of 5 wt.%VO_2/CeO_2 sample (Fig. 2), show the presence of spherical fine particles, which are gathered into larger grains that coexist with other small geometric particles. EDX analysis indicates a vanadium content of 4.89 %.

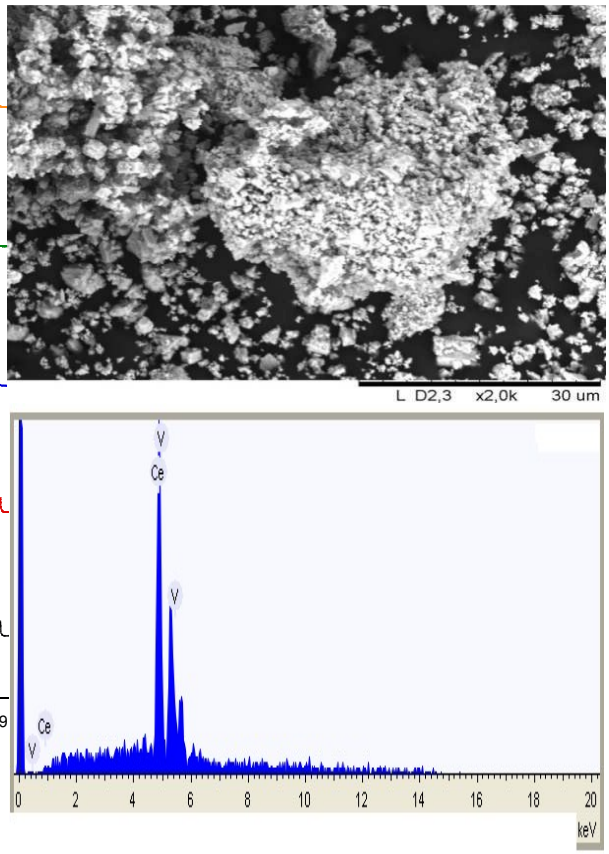

Fig. 2 SEM micrograph with EDX spectrum of 5 wt.%VO_2/CeO_2 sample.

For a comparison purpose, the experimental vanadium loading determined by atomic absorption is 5.78 %, for this same sample. The difference between these values may be explained by the fact that EDX is a very localized surface analysis while atomic absorption is a global and bulk analysis, so that if the vanadium distribution is not very homogenous, the results may differ.

3.1.4 TGA/DTA analysis

Fig. 3 illustrates the TGA/DTA analysis of 5 wt.%VO_2/CeO_2, conducted before calcination and reduction at 400°C. An

endothermic peak, observed from room temperature to 200 °C for supported catalysts, can be attributed to the removal of water [28]. The small endothermic peak at 600 °C may be attributed to the fusion of VO_2, and to the formation of $CeVO_4$ [28]. Around 950 °C, new phases may be formed [34, 35]. The total weight loss of the sample is about 3 %, in the temperature range 25 – 1200 °C.

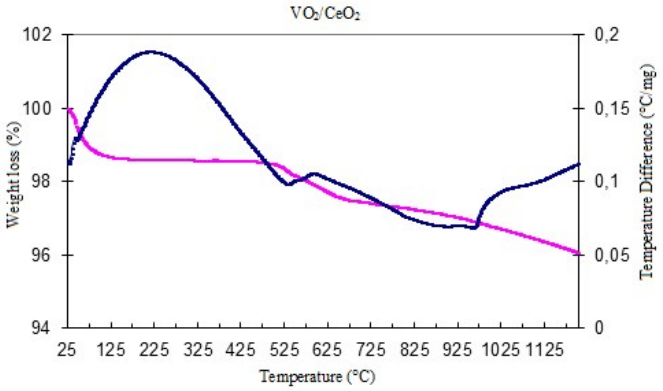

Fig. 3 Thermal gravimetric analysis of the 5wt.%VO_2/CeO_2 sample, before thermal treatment at 400 °C.

3.1.5 DR UV–vis spectroscopy

The UV-Vis DRS spectroscopy was used to investigate the structure of supported vanadia catalysts, as the ligand-to-metal charge transfer (LMCT) transitions of V^{4+} appear in the 200 – 500 nm region, and the d-d transition bands in the 600–800 nm region [36-38]. The UV-Vis spectra of the samples are shown in Fig. 4.

For clearness purposes, the attribution of the characteristic bands according to literature is reported in the following Table 3:

Table 3: attribution of UV-Vis characteristic bands according to litterature

Band (nm)	Attribution	References
225 and 278	$Ce^{3+} \leftarrow O^{-2}$ and $Ce^{4+} \leftarrow O^{-2}$ charge transfers,	18, 39, 40
240-280	Tetrahedral V^{4+} monomeric species.	41
270-300	Tetrahedral V^{5+} monomeric species.	41-46
300-350	Tetrahedral V^{5+} polymeric species.	41-44
350-400	Octahedral V^{5+} monomeric species.	41, 45-48
400-500	Octahedral V^{5+} polymeric species.	41-44, 46, 49-51
500-550	Presence of V_2O_5 crystalline.	43, 52, 53
550-800	Transition d-d of vanadium (IV).	46, 49, 52
600-800	Presence of $CeVO_4$	54

For all samples, the results indicate the presence of the d-d transition band attributed to V^{4+} cations. The bands around 225 nm and 278 nm are most likely due to $Ce^{3+} \leftarrow O^{-2}$ and $Ce^{4+} \leftarrow O^{-2}$ charge transfers, respectively [18, 39, 40]. The band of vanadium species, noted in the region 300 - 350 nm, should be assigned to charge-transfer transitions involving oxygen and vanadium (IV) in tetrahedral coordination, present as polymeric species [43, 45, 55]. The band The band in the region 400 - 500 nm is attributed to octahedral V^{4+} polymeric species [43, 56, 57]. Jian et al. [58] showed the presence of monovanadyl species for low vanadium contents (0.1 and 1 %), and the presence of polyvanadyl species for a higher vanadium content (4 %). In the case of 20 wt.% vanadium, the band of crystalline VO_2 appears at 547 nm [43, 59, 60]. Using XRD and UV-Vis, Gu et al.[31] and Duarte de Farias et al.[61] noted the presence of the V_2O_5 crystalline phase, in 20 wt.%V_2O_5/CeO_2 and 18 wt.%V_2O_5/CeO_2, respectively. The absence of crystalline VO_2 diffraction peak in the case of 20 wt.%VO_2/CeO_2 may be due to the small size crystallites, which are most likely smaller than the detection limit of the XRD technique.

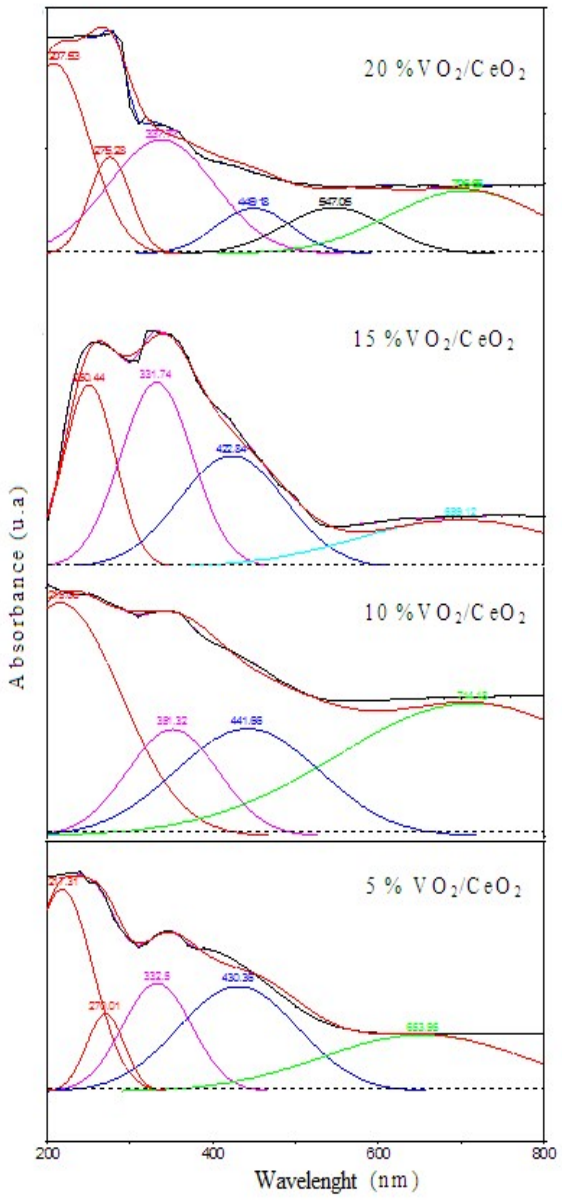

Fig. 4 Diffuse-reflectance UV-Vis deconvoluted spectra of the X wt.% VO_2/CeO_2 materials.

3.1.6 FT-IR absorption with ATR

The infrared spectra were deconvoluted by the deconvolution software PeakFit. Deconvoluted infrared spectra of VO_2/CeO_2 materials, in the 1500 – 500 cm^{-1} region, are reproduced in Fig. 5. From deconvolution, the following bands are obtained:

- ✓ between 540 and 650 cm^{-1}: attributed to the rocking modes of the V–O–V bonds [43, 62, 63],
- ✓ at 750 cm^{-1}: due to stretching vibration of the V–O–V bonds [58],
- ✓ at 870 cm^{-1}: due to V=O and V–O–V coupled vibration [61],
- ✓ around 1007 cm^{-1}: due to the asymmetric stretching vibration of the V=O bond in polyvanadate [61, 64].

In the case of 20 wt.%VO_2/CeO_2, the appearance of a new band, centered at 991 cm^{-1}, is attributed to the crystalline phase of the vanadium oxide [61, 65]. The FTIR and UV-Visible spectroscopy results are found to be in good agreement.

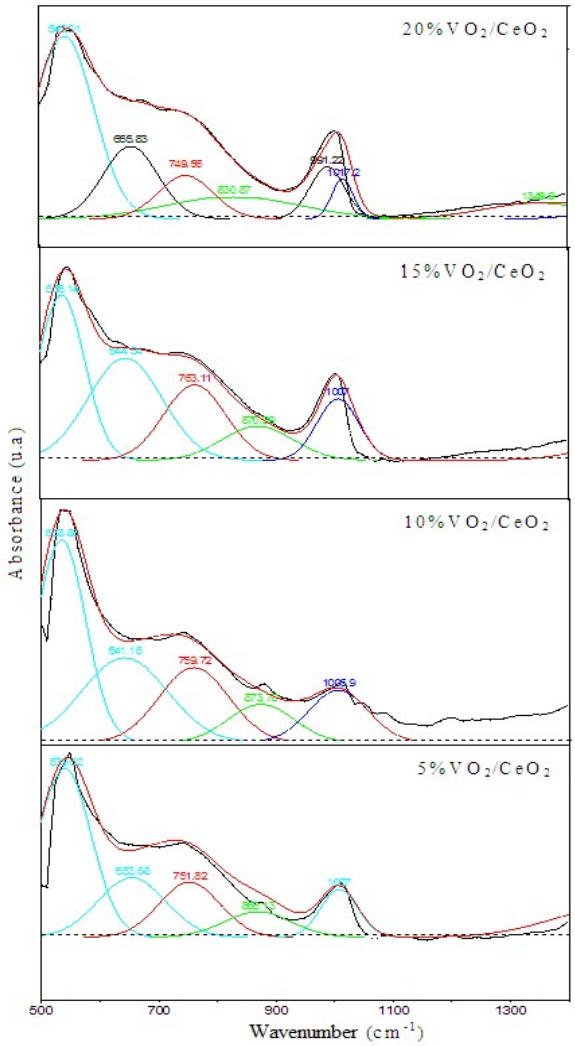

Fig. 5 Room temperature FTIR deconvoluted bands of the X wt.% VO_2/CeO_2 materials.

3.2. Catalytic activity

Generally, cyclohexane oxidation gives mainly cyclohexane oxide (epoxide), cyclohexane diols, cyclohexenol (Enol), cyclohexenone (Enone), cyclohexanol (Ol) and cyclohexanone (One) (Fig. 6) [66-69]. Oxidation of cyclohexene with TBHP, in the presence of vanadium supported oxides, resulted in the formation of several products, as shown in Table 4. Through GC analysis, 1,2-cyclohexanediol was not detected in the reaction mixture [70, 71]. In the absence of catalyst, cyclohexene gave only 12 % conversion; no epoxide was found [72]. Since the CeO_2 catalytic test gave a result similar to the one without catalyst, it can be concluded that the support was not active [31].
According to the results reported in table 4, activity decreases with increased vanadium loading; this is due to the saturation of the surface with adsorbed species, whereas the epoxide selectivity increases up to 90 % when the vanadia loading rises up to 15 wt.%. However, the 20 wt.%VO_2/CeO_2 catalyst directs the reaction towards the allylic oxidation where a selectivity of 100 % towards enol and enone is reached.

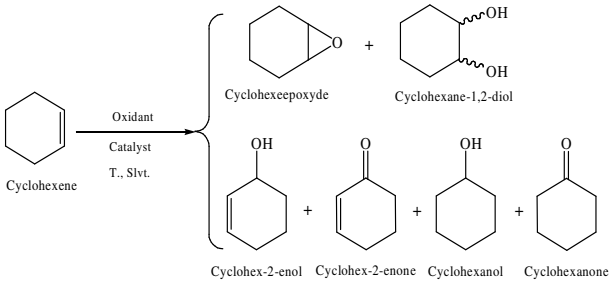

Fig. 6: Different possible products of cyclohexene oxidation reaction.

Thus, the similar surface structure as well as the similar surface acidity and redox property might be responsible for the identical behavior of these catalysts for the selective oxidation of cyclohexene. In fact, the structural characterizations given above show that 5, 10 et 15 wt.%VO_2/CeO_2 materials have only polymeric sites, while the 20 wt.%VO_2/CeO_2 catalyst possesses a signficant amount of crystalline VO_2 on the surface and exhibits a significant surface acidity [31, 73]. Consequently, this sample directs the selectivity towards cyclohexenol and cyclohexenone. There might be three types of V–O bonds in the supported VO_2 catalysts, i.e. V–O, V–O–V and V–O–support [5].

Table 4 Oxidation of cyclohexene, using different supported catalysts.

Catalysts	Activity		Selectivity (%)						TBHP consumption (%)
	Conv (%)	TOF (h^{-1})	Epoxide	Enone	One	Enol	Ol	Diol	
5%VO_2/CeO_2	45	17.1	77	18	/	5	/	/	50
10%VO_2/CeO_2	28	5.5	80	11	/	9	/	/	82
15%VO_2/CeO_2	20	3.0	90	6	/	4	/	/	68
20%VO_2/CeO_2	5	0.0	/	64	/	36	/	/	98

Reaction conditions: cyclohexene 29 mmol, TBHP 38.45 mmol, Heptane 25 mL, 0.1 g catalyst, reaction time 6 h, reaction temperature 65 °C.

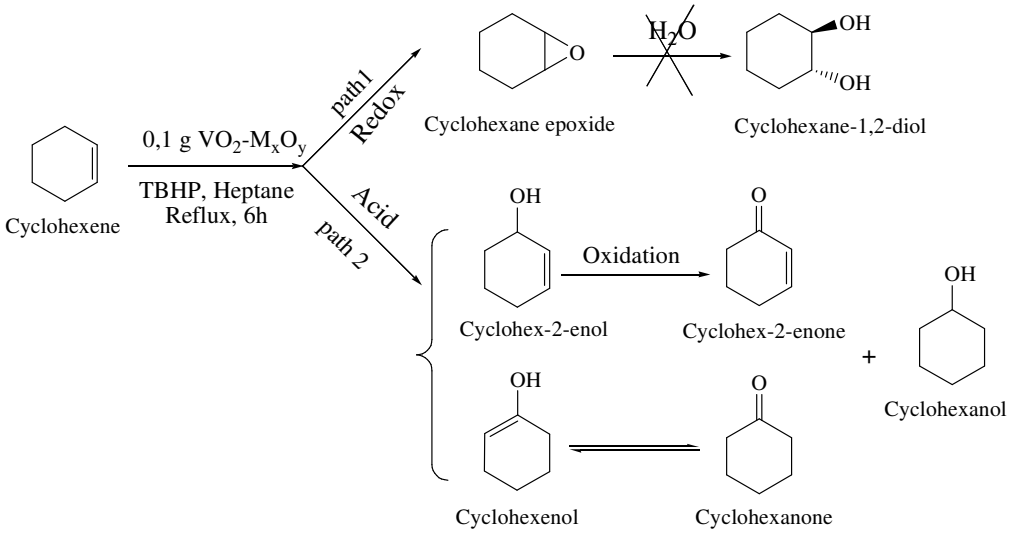

Fig. 7 Different pathways for cyclohexene oxidation reaction.

The redox property of catalysts might have mainly originated from the V–O–support bonds, instead of the V–O–V bonds, as bulk VO_2 is mainly acidic rather than redox. Weckhuysen and Keller [5] ascribed the activity of selective oxidation of methanol to formaldehyde to the V–O–support bonds in the supported vanadia catalysts, after comparing the effects of different supports. It is difficult to determine the surface density of the V–O–support bonds directly. However, it is reasonable to infer that the highest density of the surface V–O–support bonds might be reached when the loading of VO_2 is lower than the monolayer capacity, since once the loading reaches the monolayer capacity, the surface vanadium species would form a two-dimensional network in which V–O–V may be the most popular bonds.

The mechanism of the epoxidation reaction of cyclohexene with TBHP on vanadium mixed oxides was studied earlier [25] and it was shown that it occurs following two pathways: the first one is a direct epoxidation, in the presence of redox catalysts, leading to epoxide formation. The second one is an allylic oxidation in the presence of Lewis acid catalysts to give cyclohexenol, cyclohexenone, cyclohexanone and cyclohexanol.

The VO_2 loading in the 5 wt.%VO_2/CeO_2 was close to the monolayer capacity, as discussed above. This catalyst might possess the strongest redox ability among the catalysts under study in this work. In fact, it exhibits the highest activity for the selective epoxidation of cyclohexene (Fig. 7). The so-called highly dispersed vanadium species, mentioned above, can be taken as the isolated, dimeric and polymeric vanadium species. The surface V–O–Ce bonds seem to be important for the selective epoxidation of cyclohexene.

Table 5 summarizes several results reported in the literature dealing with cyclohexene epoxidation with TBHP on a wide range of vanadium based catalysts. It can be noticed that our catalysts, in particular 5 wt.% VO_2/CeO_2 are from the most interesting ones.

Table 5: Comparison of the present work with literature

Catalyst	Substrate	Activity		Epoxide selectivity (%)	Ref
		Conversion (%)	TOF (h^{-1})		
V-MCM-41	Cyclohexene ,TBHP as oxidant, chloroform as solvent, 65°C, 6h, 0.200g catalyst	27		92	74
Alumina-supported vanadyl complexes	Cyclohexene ,TBHP as oxidant, CH_2Cl_2 as solvent, reflux, 8h, 1.0g catalyst	94		0	75
V_2O_5/SiO_2	Cyclohexene, TBHP as oxidant, 80°C, 6h, 0.100g catalyst	53		0	73
Oxovanadium (VI) based coordination polymers	Cyclohexene, TBHP as oxidant, CH_3CN as solvent, 75°C, 6h, 0.015g catalyst	98		45	76
V-grafted silica sphere	Cyclohexene, TBHP as oxidant, toluene as solvent, reflux, 5h, 0.020g catalyst	63	3.9	6.2	77
Alumina- supported vanadium	Cyclohexene, TBHP as oxidant, 60°C, 5h, 0.015g catalyst	30		100	79
V_2O_5-TiO_2	Cyclohexene, TBHP as oxidant, heptane as solvent, 80°C, 6h, 0.100g catalyst	46		75	66
VO_2-SiO_2	Cyclohexene, TBHP as oxidant, heptane as solvent, 65°C, 6h, 0.100g catalyst	21		83	32
VO_2-TiO_2		13		21	
VO_2-Al_2O_3		17		0	
Vanadium-chromium-bentonite	Cyclohexene, TBHP as oxidant, heptane as solvent, 70°C, 6h, 0.100g catalyst	32		69	68

Since 5 wt.% VO_2/CeO_2 is the best catalyst, affording a high conversion to cyclohexene and a high epoxide selectivity and a high TOF, it was chosen as a standard catalyst to study the influence of varying the parameters such as catalyst amount, cyclohexene to TBHP molar ratio, thermal treatment temperature and the stability of catalyst, upon the cyclohexene oxidation reaction.

.

3.2.1. Effect of the catalyst amount

To investigate the effect of the catalyst amount for the 5 wt.%VO_2/CeO_2 sample, the following weights were considered: 0.025, 0.05, 0.1, 0.2 and 0.3 g. The results are summarized in table 6.

Table 6 Effect of catalyst amount, for 5 wt.%VO_2/CeO_2, on the epoxidation reaction of cyclohexene, with TBHP.

Catalyst amount (g)	Activity		Selectivity (%)						TBHP consumption (%)
	Conv (%)	TOF (h^{-1})	Epoxide	Enone	One	Enol	Ol	Diol	
0.025	33	46.8	72	17	7	4	/	/	48
0.05	38	28.0	75	17	5	3	/	/	53
0.1	45	17.1	77	18	/	5	/	/	50
0.2	42	7.6	74	17	5	4	/	/	57
0.3	43	4.9	70	16	8	6	/	/	65

Reaction conditions: cyclohexene 29 mmol, TBHP 38.45 mmol, Heptane 25 mL, reaction time 6 h, reaction temperature 65 °C.

Table 7 Effect of cyclohexene/TBHP molar ratio, for the 5 wt.%VO_2/CeO_2, on the epoxidation reaction of cyclohexene.

Molar ratio cyclohexene/ TBHP	Activity		Selectivity (%)						TBHP consumption (%)
	Conv (%)	TOF (h^{-1})	Epoxide	Enone	One	Enol	Ol	Diol	
1/2	48	4.5	19	16	58	7	/	/	60
1/1.3	45	17.1	77	18	/	5	/	/	50
1/1	44	18.4	85	9	/	6	/	/	40
1/0.5	18	8.4	95	2	/	3	/	/	32

Reaction conditions: cyclohexene 29 mmol, Heptane 25 mL, 0.1 g catalyst, reaction time 6 h, reaction temperature 65 °C.

From these results, TOF is seen to decrease with the amount of catalyst from 46.8 to 4.9. The selectivity to epoxide remains constant, around 77 %, regardless of the catalyst amount. When the catalyst mass is increasing, particle aggregation in the suspension might be more pronounced, resulting in poor reactant accessibility to pores, which subsequently gives a lower catalytic activity [80].

3.2.2. Effect of cyclohexene/TBHP molar ratio

The concentration of TBHP is another important parameter affecting the cyclohexene oxide selectivity. By keeping the substrate (cyclohexene) amount constant, the effect of TBHP amount was investigated over a wide range of cyclohexene to TBHP molar ratio ranging from 0.5 to 2, with 5 wt.% VO_2/CeO_2 as catalyst.

Table 7 represents the cyclohexene conversion, TOF and products selectivities at various cyclohexene/TBHP ratios, in the presence of 5 wt.%VO_2/CeO_2. As it can obviously be seen, the cyclohexene conversion decreases as the cyclohexene/TBHP molar ratio rises and the epoxide selectivity increases as this molar ratio goes up. The best cyclohexene/TBHP ratio should be 1/1.3 and 1/1 with the highest TOF. Anand et al. [81] attributed the decreasing cyclohexene conversion with the increase in cyclohexene/TBHP ratio to the fact that cyclohexene molecules occupy most of the active centers on the catalyst surface, thus leaving less space for TBHP. In our case, when the cyclohexene/TBHP molar ratio increases, there is a competition between cyclohexene and TBHP, so the more there is of cyclohexene, the less TBHP is adsorbed on the active sites, and therefore conversion decreases. However, each time a TBHP molecule is adsorbed, it reacts with the cyclohexene adsorbed on an adjacent site to form epoxide, and the selectivity increases.

3.2.3. Effect of thermal treatment

In order to check the effect of high-temperature thermal treatment, the 5 wt.%VO_2/CeO_2 catalyst, previously calcined and reduced at 400 °C, was heated again for 4h, at 800 °C, under argon flow (28 mL min^{-1}), to obtain the 5 wt.%VO_2/CeO_2 (800 °C). Catalyst 5 wt.%V_2O_5/CeO_2 was obtained from dried V/CeO_2 by calcination at 400 °C.

These different treatments result in different V oxidation states (table 8). Indeed, V oxidation state is proven by the presence or not of the d-d transition bond in the DRUV-Vis spectra (figures 4 and 8) which is only present in the case of V^{4+}.

The results of the effect of these treatments on the reaction of cyclohexene oxidation are summarized in table 8.

Results from table 7 show that the oxidation number +4 of VO_2 and +5 of V_2O_5, for the catalysts treated at 400 °C, do not induce any change in the catalytic activity of both catalysts. The redox properties of ceria (Ce^{4+}/Ce^{3+}) and the high ability of its lattice oxygen are among the most important factors that contribute to the catalytic reactivity in epoxidation reactions [18, 19, 30]. The deposition of vanadium on the surface of cerium oxide increases and improves the CeO_2 ability to provide an oxygen from its own network which will oxidize the adsorbed cyclohexene [61], according to the reaction [40]:

$$CeO_2 \rightleftharpoons CeO_{2-x} + xO_2$$

Table 8 Effect of thermal treatment on the epoxidation reaction of cyclohexene, with TBHP.

Catalysts	V oxidation state	Activity		Selectivity (%)						Consumption of TBHP (%)
		Conv (%)	TOF (h^{-1})	Epoxide	Enone	One	Enol	Ol	Diol	
$5\%V_2O_5/CeO_2$	+5	49	17.9	74	7	19	/	/	/	57
$5\%VO_2/CeO_2$	+4	45	17.1	77	18	/	5	/	/	50
$5\%VO_2/CeO_2$ (800 °C)	+4	21	5.1	49	13	31	7	/	/	22

Reaction conditions: cyclohexene 29 mmol, TBHP 38.45 mmol, Heptane 25 mL, 0.1 g catalyst, reaction time 6 h, reaction temperature 65 °C.

The 5wt.%V/CeO_2 catalysts treated at 400 °C contain the most reducible V species. Since this material contains detectable polyvanadate species (Fig. 8), it is proposed that this surface phase is responsible for cyclohexene epoxidation, and the bridging oxygen in V–O–V and V–O–Ce is most likely the key catalytic site [21]. For the 5 wt.%VO_2/CeO_2 (800 °C) catalyst, cyclohexene conversion and selectivity decrease even if epoxide remains the major product. This decrease is due to the formation of a new crystalline phase ($CeVO_4$). The XRD powder patterns (Fig. 9) of the VO_2/CeO_2 sample, treated at 800 °C, reveal, in addition to sharp ceria lines, new smaller lines which can be seen at 2θ ~ 18.33 ° and 24.06 °, respectively [ICDD pattern 12-0757]. These peaks are attributed to the formation of the CeVO4 mixed phase which is at 10 % of total CeO_2[21, 82]. However, once $CeVO_4$ was formed, the activity for the epoxidation reaction decreased. It seems that the oxygen anions in $CeVO_4$ were less active and labile than those in CeO_2 and VO_2, since they were more strongly bonded in the $CeVO_4$ lattice. The reason may be simple; the valent states of Ce and V are relatively stabilized at +3 and +5, respectively, in $CeVO_4$, leading to the weakened redox ability of $CeVO_4$. Therefore, the catalyst with abundant surface of $CeVO_4$ exhibited low activity for the epoxidation of cyclohexene [31].

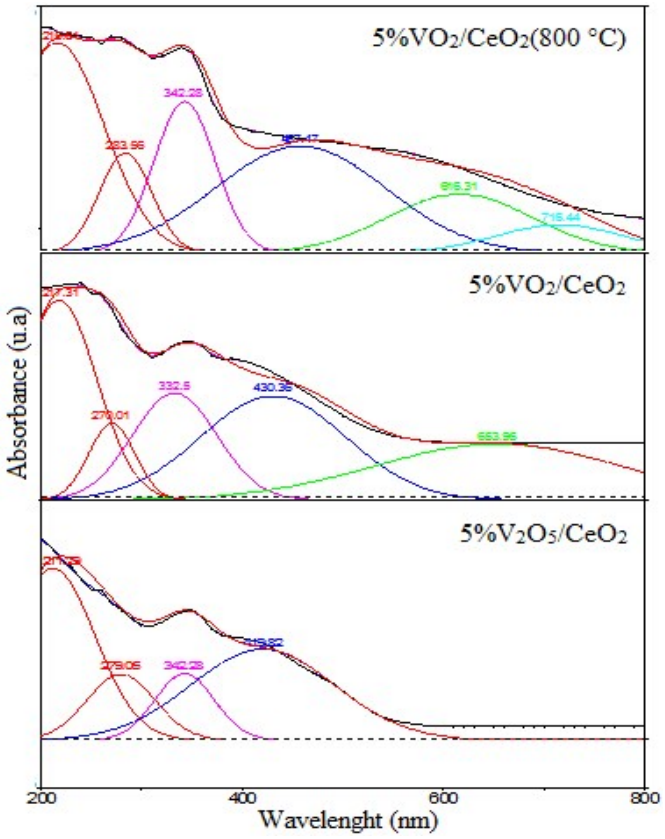

Fig. 8 Deconvoluted DR-UV-vis spectrum of 5 wt.%V_2O_5/CeO_2 material.

3.2.4 Leaching and stability

Leaching was carried out to see whether the passage of the catalyst into the organic liquid phase occurs or not. For this, reactions of cyclohexene in the presence of the catalyst 5 wt.%VO_2/CeO_2 were studied. After 6 h of reaction time, the organic phase and the solid phase were separated by filtration. The reaction of the organic phase was started again for 2 hours, adding an amount of each reactant and heating to reflux temperature. The results of this reaction showed that no epoxide was produced; similar results were reported by Brutchey et al.[83] and Farzaneh et al.[74]. In addition, it was noted that the solution remains clear in the presence of TBHP and cyclohexene[77]. It can be stated from these results that no catalyst leaching occurs, and the reaction is really heterogeneous.

The results of the stability of catalyst 5 wt.%VO_2/CeO_2 during the epoxidation reaction of cyclohexene are shown in table 9. They indicate that this material is stable during 3 cycles of the reaction.

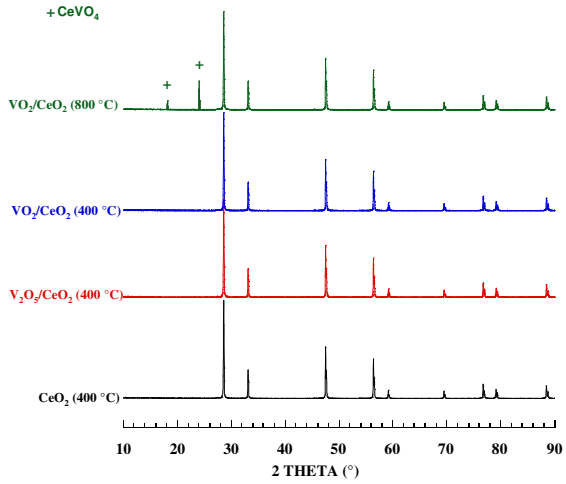

Fig. 9: X-ray diffraction (XRD) patterns of V_xO_y/CeO_2 systems, upon different thermal treatments.

Table 9 Results of the stability of 5 wt.%VO_2/CeO_2 during the epoxidation reaction of cyclohexene with TBHP.

Cycle	Conversion (%)	Epoxide Selectivity (%)	TOF (h^{-1})	TBHP Consumption (%)
1st	45	77	17.1	50
2nd	46	75	17.0	54
3rd	43	73	15.5	28
4th	18	42	3.7	25

Reaction conditions: cyclohexene 29 mmol, TBHP 38.45 mmol, Heptane 25 mL, 0.1 g catalyst, reaction time 6 h, reaction temperature 65 °C.

4. Conclusions

The X wt.% VO_2/CeO_2 supported oxide materials were prepared by the impregnation method. They were then calcined and reduced at 673 K. The materials obtained had a green color, which indicates the presence of reduced vanadium (IV) species. The XRD results revealed that VO_2 is dispersed on the ceria surface. The surface of supported oxides decreases with increasing vanadia loading. As it has been previously confirmed by FTIR results, UV-Vis spectra of the samples showed that vanadyl species are incorporated in the carrier in polymer form; in the case of 20 % by weight of vanadium, the crystalline VO_2 band appears. VO_2/CeO_2 system has proven to be an efficient catalyst for the selective epoxidation of cyclohexene, with TBHP as oxidant and heptane as solvent. The optimum operating conditions are 0.025 g catalyst, cyclohexene/TBHP = 1/1 at 65°C and 6h reaction. The cyclohexene conversion decreased with increased vanadium loading; whereas the epoxide selectivity increased up to 90 % with increasing vanadia loading up to 15 wt.%. The 20 wt.%VO_2/CeO_2 catalyst directed the reaction towards the allylic oxidation, with 100 % selectivity toward enol and enone. For the 5 wt.%VO_2/CeO_2 (800 °C) catalyst, the conversion and selectivity of cyclohexene decreased due to the presence of $CeVO_4$ as a new crystalline phase. Epoxide remained the major reaction product.

From all these cyclohexene oxidation results, it was evidenced that in the presence of redox catalysts, this reaction leads to an epoxidation product, while in the presence of acidic features, the allylic oxidation is preponderant and leads to cyclohexenol and cyclohexenone.

Acknowledgements

The authors would like to thank the *General Directorate for Scientific Research and Technological Development* (DGRST) as well as the *Thematic Agency* for *Research* in *Science and Technology* (ATRST) for the financial support to the project *rtn-tr010* Pro Thème/56/2015.

References

1. M. Dusi, T. Mallat and A. Baiker, *Catal. Rev.*, 2000, **42**, 213-278.
2. J.Gao , Y.Chen , B. Hau , Z. Feng , C. Li , N. Zhou , S. Gao and Z. Xi, *J. Mol. Cat. A*, 2004, **210**, 197.
3. H. Vrubel, K. J. Ciuffi, G. P. Ricci, F. S. Nunes and S. Nakagaki, *Appl. Catal. A*, 2009, **368**, 139-145.
4. T. Kim and I. E. Wachs, *J. Catal.*, 2008, **255**, 197-205.
5. B. M. Weckhuysen and D. E. Keller, *Catal. Today*, 2003, **78**, 25-46.
6. T. Radhika and S. Sugunan, *Catal. Comm*, 2007, **8**, 150-156.
7. X. Gao, J-M. Jehng and I. E. Wach, *J. Catal.*, 2002, **209**, 43-50.
8. N. Ballarini, F. Cavani, M. Ferrari, R. Catani and U. Cornaro, *J. Catal.*, 2003, **213**, 95.
9. G. C. Bond and S. F. Tahir, *Appl. Catal.*, 1991, **71**, 1-31.
10. I.E. Wachs, *Chem. Eng. Sci*, 1990, **45**, 2561.
11. H. Zou, M. Li, J. Shen and A. Aroux, *J. Therm. Anal. Calori*, 2003, **72**, 209-221.
12. T. Kataoka and J.A. Dumesic, *J. Catal.*, 1988, **112**, 66.
13. F.Arena, F.Frusters and A. Parmaliana, *Appl. Catal. A*, 1999, **176**, 189-199.
14. G.T. Went, S.T. Oyama and A.T. Bell, *J. Phys. Chem.*, 1990, **94**, 4240.
15. A. Khodakov, B. Olthof, A.T. Bell and E. Iglesia, *J. Catal.*, 1999, **181**, 205-216.
16. S. Bedrane, C. Descorme and D. Duprez, *Catal. Today*, 2002, **75**, 401-405.
17. A.Trovarelli, *Catalysis by ceria and related materials*, Catalytic Science series edn., Imperial College Press, London, UK, 2002.
18. M. M. Mohamed and S. M. A. Katib, *Appl. Catal. A*, 2005, **287**, 236-243.
19. S. Bedrane, C. Descorme and D. Duprez, *Appl. Catal. A*, 2005, **289** 90-96.
20. M.A. Bañares, X. Gao, J.L.G. Fierro and I.E. Wachs, *Stud. Surf. Sci. Catal.*, 1997, **110**, 295.
21. W. Daniell, A. Ponchel, S. Kuba, F. Anderle, T. Weingand, D. H. Gregory and H. Knozinger, *Top. Catal.*, 2002, **20**, 65-74.
22. M. V. Martínez-Huerta, J. M. Coronado, M. Fernández-García, A. Iglesias-Juez, G. Deo, J. L.G. Fierro and M. A. Bañares, *J. Catal.*, 2004, **225**, 240-248.
23. M.A. Bañares, M.V. Martínez-Huerta, X. Gao, I.E. Wachs and J.L.G.Fierro, *Stud. Surf. Sci. Catal.*, 2000, **130**, 3125.
24. A.R. González-Elipe and F. Yubero, *Surface and Interface Analysis and Properties, in: Handbook of Surfaces and Interfaces of Materials, p 147.*, H.S. Nalwa edn., Academic Press, San Diego, 2001.
25. S. El-Korso, I. Khaldi, S.Bedrane, A.Choukchou-Braham, F. Thibault-Starzyk and R. Bachir, *J. Mol. Cat. A*, 2014, **394** 89-96.
26. S. Bedrane, C. Descorme and D. Duprez, *J. Mater. Chem.*, 2002, **12**, 1563-1567.
27. R. Neumann and M. Levin-Elad, *Appl. Catal. A*, 1995, **122**, 85-97.
28. T. Radhika and S. Sugunan, *J. Mol. Cat. A*, 2006, **250**, 169-176.
29. S. Bedrane, C. Descorme and D. Duprez, *Stud. Surf. Sci. Catal.*, 2001, **138**, 125-134.
30. T. Radhika and S. Sugunan, *Catal. Commun.*, 2007, **8**, 150-156.
31. X. Gu, J. Ge, H. Zhang, A. Auroux and J. Shen, *Thermochimica Acta*, 2006, **451**, 84-93.
32. S. EL-KORSO, I. REKKAB, A. CHOUKCHOU-BRAHAM, S. BEDRANE, L. PIRAULT-ROY and C. KAPPENSTEIN, *Bull. Mater. Sci.*, 2012, **35**, 1187-1194.
33. F. Arena, F. Frusteri and A. Parmaliana, *Cat. Lett.*, 1999, **60**, 59-63.
34. C. Pallazi, L. Oliva, M. Signoretto and G. Strukul, *J. Catal.*, 2000, **194**, 286-293.
35. H. Zou and Y. S. Lin, *Appl. Catal. A*, 2004, **265**, 35-42.
36. H.Feng, J. W.Elam, J. A.Libera, M. J.Pellin and P. C.Stair, *Journal of Catalysis*, 2010, **269**, 421-431.
37. J. Liu, Z. Zhao, C. Xu, A. Duan and G. Jiang, *J. Rare Earths*, 2010, **28**, 198-204.
38. K.Wu, B. Li, C.Han and J.Liu, *Applied Catalysis A: General*, 2014, **479**, 70-75.
39. M. I. Zaki, G. A. M. Hussein, r. S. A. A. Mansou, H. M. Ismail and G. A. H. Mekhemer, *Coll. Surf. A*, 1997, **127**, 47-56.
40. M.A. Centeno, M. Paulis, M. Montes and J.A. Odriozola, *Appl. Catal. A*, 2002, **234**, 65-78.

41. V. Murgia, E. M. F. Torres, J. C. Gottifredi and E. L. Sham, *Appl. Catal. A: Gen*, 2006, **312**, 134-143.
42. R. Monaci, E. Rombi, V. Solinas, A. Sorrentino , E. Santacesaria and G. Colon, *Appl. Catal. A: Gen*, 2001, **214**, 203-212.
43. V. Iannazzo, G. Neri, S. Galvagno, M. Di Serio, R. Tesser and E. Santacesaria, *Appl. Catal. A: Gen*, 2003, **246**, 49-68.
44. P. Concepcion, M. Navarro, T. Blasco, J. Lopeznieto, B. Panzacchi and F. Rey, *Catal. Today*, 2004, **96**, 179-186.
45. F. Ke-gong, W. Bin and S. Yu-han, *Chem. Res. Chin. Univ*, 2009, **26**, 924-928.
46. A. Held, J. Kowalska-Kuś and K. Nowińska, *Catal. Comm*, 2012, **17**, 108-113.
47. T. Blasco, A. Galli, J. M. L. Nieto and F.Trifiro, *J. Catal*, 1997, **169**, 203-211.
48. K. V. R.Chary, C. P. Kumar, D. Naresh, T. Bhaskar and Y. Sakata, *J. Mol. Catal. A: Chem*, 2006, **243**, 149-157.
49. M. A. Figueiredo, A. Luis de Faria, M. das D. Assis and H. P. Oliviera, *J. Non-Crys. Sol*, 2005, **351**, 3624-3629.
50. F. Adam, T-S. Chew and J. Andas, *Chin. J. Catal*, 2012, **33**, 518-522.
51. L. Dong, C. Sun, C. Tang, B. Zhang, J. Zhu, B. Liu, F. Gao, Y. Hu, L. Dong and Y. Chen, *Appl. Catal. A: Gen*, 2012, **431-432**, 126-136.
52. D. E. Keller, T. Visser, F. Soulimani, D.C. Koningsberger and B. M. Weckhuysen, *Vib. Spect*, 2007, **43**, 140-151.
53. F. M. Bautista, J. M. Campelo, D. Luna, J. Luque and J. M. Marinas, *Appl. Catal. A: Gen*, 2007, **325**, 336-344.
54. Z. Wu, A. J. Rondinone, I. N. Ivanov and S. H. Overbury, *J. Phys. Chem. C*, 2011, **115**, 25368-25378.
55. Y-M. Liu, Y. Cao, N. Yi, W-L. Feng, W-L. Dai, S-R. Yan, H-Y. He and K-N. Fan, *J. Catal.*, 2004, **224**, 417-428.
56. R. Monaci, E. Rombi, V. Solinas, A. Sorrentino , E. Santacesaria and G. Colon, *Appl. Catal. A*, 2001, **214**, 203-212.
57. V. Murgia, E. M. F. Torres, J. C. Gottifredi and E. L. Sham, *Appl. Catal. A*, 2006, **312**, 134-143.
58. J. Liu, Z. Zhao, C. Xu, A. Duan and G. Jiang, *J. Rare Earth.*, 2010, **28**, 198-204.
59. D. E. Keller, T. Visser, F. Soulimani, D.C. Koningsberger and B. M. Weckhuysen, *Vib.Spect.*, 2007, **43**, 140-151.
60. F. M. Bautista, J. M. Campelo, D. Luna, J. Luque and J. M. Marinas, *Appl. Catal. A*, 2007, **325**, 336-344.
61. A. M. Duarte de farias, P. Bargiela, M. Rocha and M. Fraga, *J. Catal.*, 2008, **260**, 93-102.
62. A. Comite, A. Sorrentino, G. Capannelli, M. Di Serio, R. Tesser and E. Santacesaria, *J. Mol. Cat. A*, 2003, **198**, 151-165.
63. G. N. Barbosa and H. P. Oliveira, *J. Non-Crystal. Sol.*, 2006, **352**, 3009-3014.
64. K.V. Narayana, B. D. Raju, S. K. Masthan, V. V. Rao, P. K. Rao and A. Martinn, *J. Mol. Cat. A*, 2004, **223**, 321-328.
65. Z. Elassal, L. Groula, K. Nohair, A. Sahibed-dine, R. Brahmi, M. Loghmarti, A. Mzerd and M. Bensitel, *Arab. J. Chem.*, 2011, **4**, 313-319.
66. D. Lahcene, A. Choukchou-Braham, C. Kappenstein and L. Pirault-Roy, *J.Sol-Gel. Sci. Tech*, 2012, **64**, 637-642.
67. A. Dali, I. Rekkab-Hammoumraoui, A. Choukchou-Braham and R. Bachir, *RSC. Adv*, 2015, **5**, 29167-29178.
68. N. Belaidi, S. Bedrane, A. Choukchou-Braham and R. Bachir, *Applied Clay Science*, 2015, **107**, 14-20.
69. S. Boudjema, E. Vispe, A. Choukchou-Braham, J. A. Mayoral, R. Bachir and J.M. Fraile, *RSC Advances*, 2015, **5**, 6853-6863.
70. J. Jiang, K. Ma, Y. Zhen, S. Cai, R. Li and J. Ma, *Cat. Lett.*, 2009, **131**, 105-113.
71. N. Ameur, S. Bedrane, R. Bachir and A. Choukchou-Braham, *J. Mol. Cat. A*, 2013, **374-375**, 1-6.
72. C. Yuan, Y. Zhang and J. Chen, *Chin. J. Catal*, 2011, **32**, 1166-1172.
73. S. Martınez-Méndez, Y. Henrıquez, O. Dominguez, L. D'Ornelas and H. Krentzien, *J. Mol. Catal. A: Chem*, 2006, **252**, 226-234.
74. F. Farzaneh, E. Zamanifar and C. D. Williams, *J. Mol. Catal. A: Chem*, 2004, **218**, 203-209.
75. M. Salavati-Niasari, M. R. Elzami, M. R. Mansournia and S. Hydarzadeh, *J. Mol. Catal. A: Chem*, 2004, **221**, 169-175.
76. M. R. Maurya and A. Kumar, *J. Mol. Catal. A: Chem*, 2006, **250**, 190-198.
77. D. P. Das and K. M. Parida, *Catal. Lett*, 2009, **128**, 111-118.
78. S.Tangestaninejad, M. Moghadam, V. Mirkhani, I. Mohammadpoor-Baltork, E. Shams and H. Salavati, *Catal. Comm*, 2008, **9**, 1001-1009.
79. E. Mikolajska, V. Calvino-Casilda and M. A. Bañares, *Appl. Catal. A: Gen*, 2012, **421-422**, 164-171.
80. T. Sreethawong, Y. Yamada, T. Kobayashi and S. Yoshikawa, *J. Mol. Cat. A*, 2006, **248**, 226-232.
81. C. Anand, P. Srinivasu, G. P. Mane, S. N.Talapaneni, D. S. Dhawale, M. A. Wahab, S. V. Priya, S. Varghese, Y. Sugi and A. Vinu, *Micropor. Mesopor. Mat.*, 2012, **160**, 159-166.
82. G. S. Wong and J. M. Vohs, *Surf. Sci.*, 2002, **498**, 266-274.
83. R. L. Brutchey, B. V. Mork, D. J. Sirbuly, P. Yang and T. D. Tilley, *J. Mol. Cat. A*, 2005, **238**, 1-12.

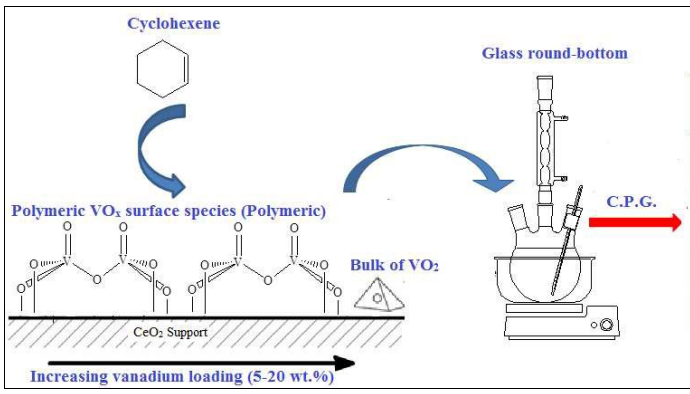

Catalysts	Conversion (%)	Selectivity (%)						TBHP consumption (%)
		Epoxide	Enone	One	Enol	Ol	Diol	
5%VO_2/CeO_2	45	77	18	/	5	/	/	50
10%VO_2/CeO_2	28	80	11	/	9	/	/	82
15%VO_2/CeO_2	20	90	6	/	4	/	/	68
20%VO_2/CeO_2	5	/	64	/	36	/	/	98

Reaction conditions: Cyclohexene 29mmol: TBHP 38.45mmol
Heptane 25mL; 0.1g catalyst; 6h; reaction temperature 65 °C.